Study on Vehicle-Induced Dynamic Response under Seasonal Temperature Variations

Qi Zhang, Xiaomin Huang*

School of Architecture and Engineering, Kunming University of Science and Technology, Kunming 650500, Yunnan, China

*E-mail: zhangqi77@stu.kust.edu.cn

Abstract. Although research on vehicle-bridge coupling during passage over expansion joints is relatively mature, the impact of seasonal temperature variations on the dynamic response of these joints has not been sufficiently explored. To address this gap, this study conducted a year-long real-time monitoring of the dynamic response of expansion joints induced by vehicle passage on a specific bridge. By analyzing the monitoring data alongside the bridge's thermal expansion coefficient, the study identified the changes in main girder and expansion joint widths due to seasonal temperature shifts, as well as the differences in equivalent force distribution coefficients under varying joint widths. Results indicated that seasonal temperature changes had minimal impact on vertical acceleration responses. However, the dynamic deflection responses exhibited periodic fluctuations with a lag effect. The deflection changes were highly synchronous across different measurement points, with mid-span deflection fluctuations being more pronounced than at the ends. In summer, the main girder lengthens, reducing the joint width to a minimum, resulting in the lowest equivalent force distribution coefficients and dynamic deflection amplitudes; conversely, winter saw maximum dynamic deflection amplitudes. Understanding the contribution of seasonal temperatures to dynamic responses is crucial for accurately assessing changes in bridge expansion joint responses.

Keywords: Seasonal Temperature Variation, Joint Width, Vehicle-Induced Joint Passage, Dynamic Deflection, Acceleration

1 Introduction

1.1 Research Background

Seasonal temperature variations lead to the thermal expansion and contraction of materials, which causes linear expansion in bridge structures. Research has shown that, aside from ground deformation, the primary factor influencing bridge deformation is the thermal expansion and contraction of construction materials. The expansion and contraction deformations caused by temperature differences fluctuate cyclically with seasonal temperature changes, and the deformation curve shows a strong correlation with the sinusoidal and cosine trigonometric functions [1].

Y. Qiu et al. (eds.), *Proceedings of the 2024 7th International Conference on Civil Architecture, Hydropower and Engineering Management (CAHEM 2024)*, Advances in Engineering Research 256,
https://doi.org/10.2991/978-94-6463-650-5_40

Expansion joints are typically used to accommodate these deformations. In the research of expansion joints, Hou et al. [2] conducted an investigation and measurement of common defects in large-span CFST arch bridges, and their research indicated that expansion joint defects can significantly increase vehicle-induced vibrations, leading to damage in components such as bearings. El-Feky et al. [3] investigated the expansion joints of bridges subjected to seismic loads, utilizing shape memory alloy (SMA) dampers as energy dissipation devices. By controlling the width of the expansion joints, they enhanced the seismic performance of the joints. Ji Wei et al. [4] conducted a numerical study on the fatigue impact factors of key structural details near the expansion joints of a composite steel box girder bridge with modified corrugated steel webs, using a vehicle-bridge coupling vibration system (VBCVS). Their results indicate that the deterioration of pavement roughness (PRC) is a key factor affecting impact modification (IM), rather than vehicle speed or the deterioration of the expansion joints (EJDD).Liang et al [5]. built a seasonal deformation model combined with time-series InSAR technology to monitor the deformation of a large bridge, successfully isolating the linear deformation caused by ground settlement from the thermal expansion and contraction induced by temperature variations. Li et al. [6] demonstrated a successful method for separating temperature effects in bridge deflection monitoring data by integrating variational mode decomposition (VMD) with K-L divergence. Shen et al. [7] observed that in a vehicle-bridge coupling vibration analysis method accounting for pavement irregularities, higher vehicle speeds exacerbate spatial vibration response issues within the vehicle-bridge system. Additionally, variations in the width of expansion joints significantly affect the vehicle-bridge coupling dynamic response, with a more pronounced impact on the dynamic response of the main girder and adjacent areas [8]. Xie et al. [9] utilized a spring-damper element model to study the vehicle-induced impact on expansion joints under conditions of pavement irregularity, examining the influence of different modular expansion joint types and gap widths on vehicle loads.

Existing research primarily focuses on the damage of expansion joints and their impact on vehicle passage, but has not addressed the characteristics and causes of dynamic responses of modular expansion joints induced by vehicles as they vary with seasonal temperature changes, particularly under different equivalent force distribution coefficients for varying joint widths. To fill this gap, this paper derives the equivalent force distribution coefficients for joint widths of 100mm, 80mm, 60mm, and 40mm, and establishes a comprehensive monitoring system to study the seasonal temperature variation in dynamic responses when wheels pass over the expansion joints. The results clarify the influence of seasonal temperature on the response of bridge expansion joints, enhance the reliability of assessments, and provide references for vehicle-joint-bridge coupling vibration response analysis.

1.2 Project Overview

The Xinmang Street Ferry Bridge in Fengqing County, Yunnan, spans the Lancang River and features a large-scale structure composed of 3×50m T-beams, a continuous rigid frame section measuring (116+220+116)m, and 4×50m T-beams. The total length of the bridge is 802m, with a width of 9.0m. At each end, the bridge is equipped with

D160 GQF expansion joint devices, allowing for a movement range of 0–160mm and a single joint width of 0–80mm. The central and edge beams of the expansion joint measure 9m in length, with the central beam constructed from I-beams and the edge beams from Z-beams. There are a total of seven supporting crossbeams, each 0.48m long and spaced 1.5m apart. The arrangement of the modular expansion joints and the overall bridge layout is illustrated in Fig**. 1.**

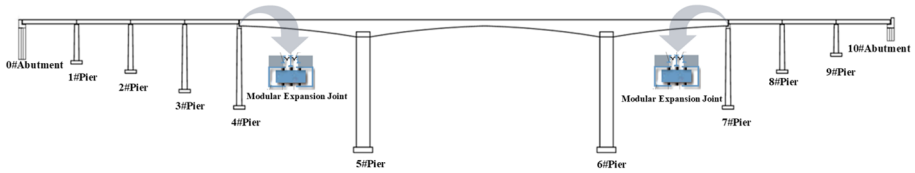

Fig. 1. Schematic diagram of the modular expansion joint and overall bridge layout

2 Design Plan

2.1 Vehicle Crossing Process Over Expansion Joints

Based on the structural form of the modular expansion joint, when a vehicle crosses the joint, the forces on each beam of the joint are closely related to the contact area of the tires. The model of a vehicle crossing the joint is shown **Fig. 2**, where s_0 represents the joint width, s is the longitudinal width of the tire, l_c is the width of the central transverse beam of the expansion joint, l_0 is the width of the edge transverse beam, and L_1 is the distance before the bridge.

According to the Highway Engineering Technical Standards, when calculating the ultimate limit state of components and connecting elements, vehicle loads are determined in accordance with the provisions outlined in the General Code for Design of Highway Bridges and Culverts (JTGD60—2015) [10]. Based on these regulations, the contact surface length s of the tire is taken as 0.2 meters.

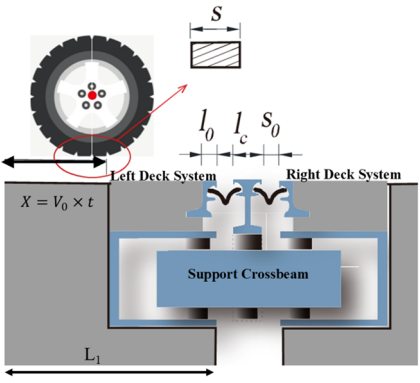

Fig. 2. Vehicle-Crossing-Joint Model

Due to the influence of the longitudinal contact length of the tire, the forces on each beam when a vehicle crosses the joint vary under different joint widths. There are two scenarios:

a) When the longitudinal contact length of the tire is relatively small, and the gap is relatively large, i.e.$s < 2s_0 + l_c$, the tire can make contact solely with the central beam of the expansion joint.

b) When the longitudinal contact length of the tire is relatively large, and the gap is relatively small, i.e. $s \geq 2s_0 + l_c$, the tire cannot solely contact the central beam of the expansion joint.

Therefore, it is necessary to discuss the vehicle crossing process under the two aforementioned conditions. Based on the vehicle crossing process [11], the equivalent force distribution coefficient is improved by incorporating the left and right bridge deck systems into the load distribution. Assuming the total wheel load on the bridge is F, during the vehicle crossing process, F_z、F_{BL1} represent the forces exerted by the wheel on the small pier-side bridge deck system and edge beam, respectively. F_{ZL} represents the force exerted on the central beam, while F_{BL2} and F_y represent the forces on the large pier-side edge beam and bridge deck system during the vehicle crossing. The equivalent force distribution coefficients for each component under different joint widths are shown in **Fig. 3**.

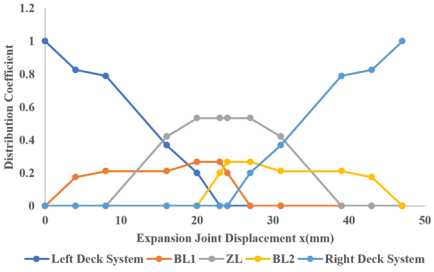

Single Wheel Load Distribution Coefficient at a Joint Width of 40mm

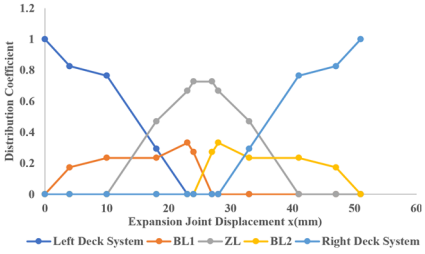

Single Wheel Load Distribution Coefficient at a Joint Width of 60mm

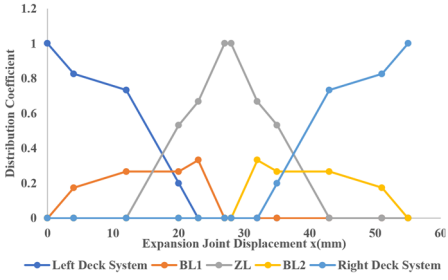

Single Wheel Load Distribution Coefficient at a Joint Width of 80mm

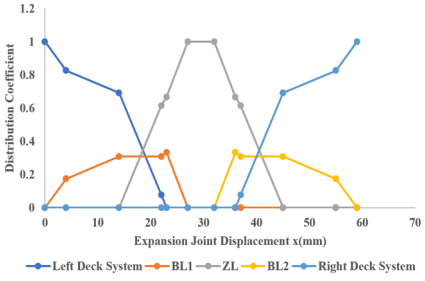

Single Wheel Load Distribution Coefficient at a Joint Width of 100mm

Fig. 3. Equivalent Force Distribution Coefficients for Expansion Joints under Different Joint Width Conditions

As shown in the figure above, the use of equivalent force distribution coefficients effectively captures the wheel load distribution during the vehicle crossing process under different joint width conditions. This parameter can be employed in subsequent analyses of the dynamic response of expansion joints with varying widths due to seasonal temperature changes, as well as in solving the force balance equations for vehicle-bridge-expansion joint coupling systems during the vehicle crossing process.

2.2 Monitoring Scheme Design

This study employs a comprehensive monitoring and analysis approach, including theoretical derivation, data collection from the monitoring system, dynamic response analysis, and correlation analysis. These methods effectively reflect the complex relationship between seasonal temperature variations and the dynamic responses of bridge expansion joints.

The dynamic deflection and vertical acceleration measurement points for the central beam of the expansion joint are arranged at the left side of the joint at P1 and at the mid-span P2. The monitoring period is from January 2023 to January 2024. The specific layout of the measurement points is shown in **Fig. 4**. The sensor details are listed in **Table 1**.

Table 1. Sensor Quantities

Measurement Items	Temperature	Dynamic Deflection	Vertical Acceleration
Sensor Types	Fiber Bragg Grating Thermometer	Fiber Bragg Grating Displacement Sensor	Fiber Bragg Grating Acceleration Sensor
Range	-40℃~120℃	5mm	±2G
Accuracy	±0.5℃	0.3mm	±0.05G
Frequency	1 hour per instance	0.2 hour per instance	0.5~120HZ
Size	Φ9×100mm	145×100×27mm	Φ73×24mm
Quantity	1unit	2unit	2unit
Installation Location	Bridge Site	Measurement Points P1 and P2	Measurement Points P1 and P2

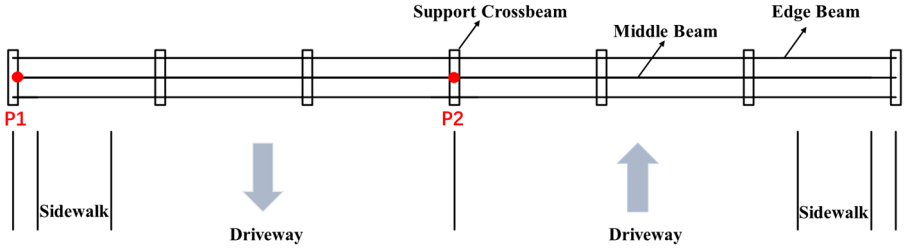

Fig. 4. Measurement Point Layout Diagram

3 Results and Analysis

3.1 Seasonal Temperature Variation

Full Period Temperature Variation Analysis. The temperature considered in this study accounts for the seasonal overall temperature rise and fall, assuming uniform temperature changes across all sections of the bridge and modular expansion joints. Temperature data for the bridge site over the entire monitoring period were compiled to obtain annual and seasonal temperature variations, as shown in **Fig. 5** and **Fig. 6**.

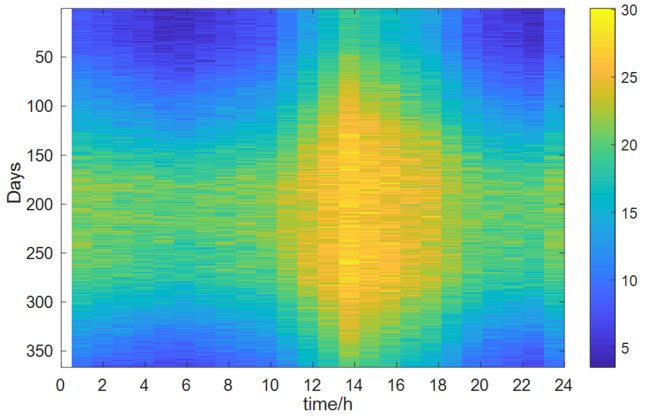

Fig. 5. Annual Temperature Variation Chart

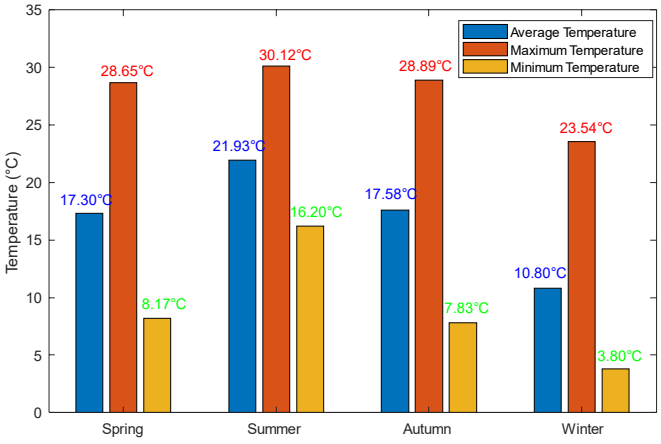

Fig. 6. Seasonal temperature chart

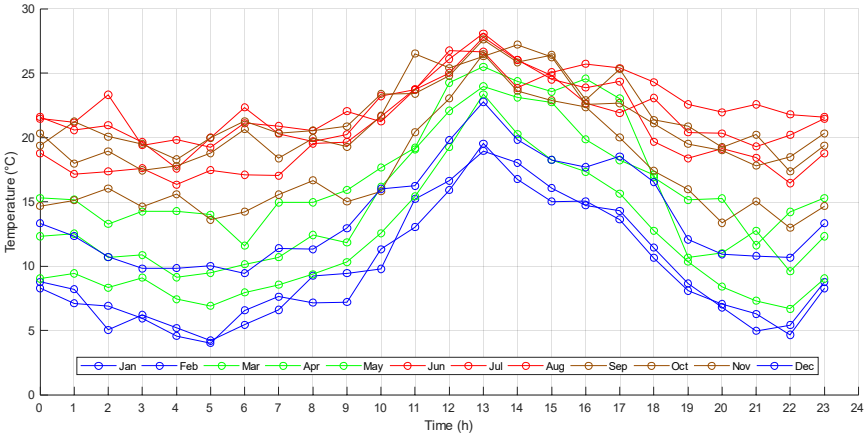

Fig. 7. Seasonal 24-Hour Temperature Variation Curves

As shown in **Fig. 7**, Spring temperatures range from 10°C to 25°C, peaking around 25°C during the day and dropping to nearly 10°C at night. Summer is notably warmer, with temperatures fluctuating between 20°C and 30°C, reaching close to 30°C at midday and remaining above 15°C at night, resulting in significant daytime variation. Autumn temperatures are similar to spring, ranging from 10°C to 25°C, with slightly greater daily fluctuations and afternoon highs near 25°C, while nighttime temperatures decrease minimally. Winter is the coldest, with temperatures between 5°C and 15°C, dipping to about 5°C in the early morning and rising to approximately 20°C during the day, exhibiting the least variation. Overall, summer has the highest and most variable temperatures, while winter is the lowest and least variable. Spring and autumn feature moderate and stable temperatures, with typical daily cycles peaking at midday and reaching their lows in the early morning.

Expansion of the Main Beam and Changes in Joint Width. The continuous rigid frame bridge being studied has a length of 452 meters. with an initial construction temperature of 10°C. The long-term linear thermal expansion coefficient of the bridge superstructure (caused by seasonal temperature differences) ranges from $3.3\sim9.1\times10^{-6}$/°C [12]. For large-span continuous rigid frame bridges, a coefficient of 8.7×10^{-6}/°Cis used. Seasonal maximum, minimum, and average temperatures obtained from monitoring are shown in **Fig. 5**, Representative temperatures are selected from the full monitoring cycle, and a baseline temperature-displacement relationship (TDR) model can be established using typical correlated temperatures. The expansion of the main beam for spring, summer, autumn, and winter is calculated as ΔL, as shown in **Fig. 8**. The calculated width of the modular expansion joints W is shown in **Fig. 9**. The calculation process is detailed in **Table 2**.

Table 2. Main Beam Contraction and Joint Width Variation Due to Seasonal Temperature Differences

Calculated Values	Spring	Summer	Autumn	Winter
ΔT_1	18.65 °C	20.12 °C	18.89 °C	13.54 °C
ΔL_1	73.3 mm	79.1 mm	74.3mm	53.2mm
W_1	116.7mm	119.6mm	117.1mm	106.6mm
ΔT_2	−1.83 °C	6.20 °C	−2.17 °C	−6.20 °C
ΔL_2	−7.2mm	24.4mm	−8.5mm	−24.4mm
W_2	76.4mm	92.2mm	75.7mm	67.8mm
ΔT_{ava}	7.30°C	11.93°C	7.58°C	0.80°C
ΔL_{ava}	28.7mm	46.9mm	29.8mm	3.1mm
W_{ava}	94.4mm	103.5mm	94.9mm	81.6mm

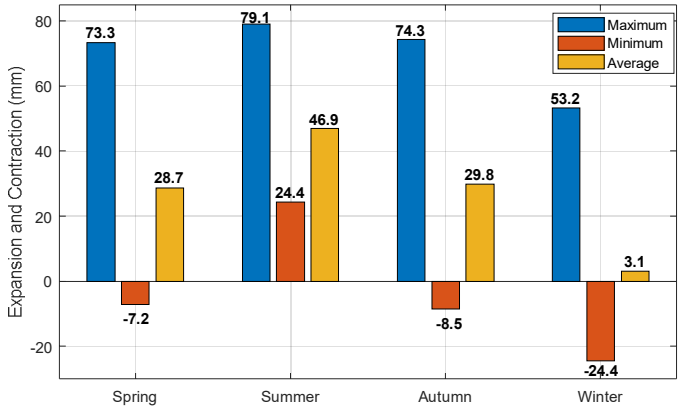

Fig. 8. Main Beam Expansion and Contraction

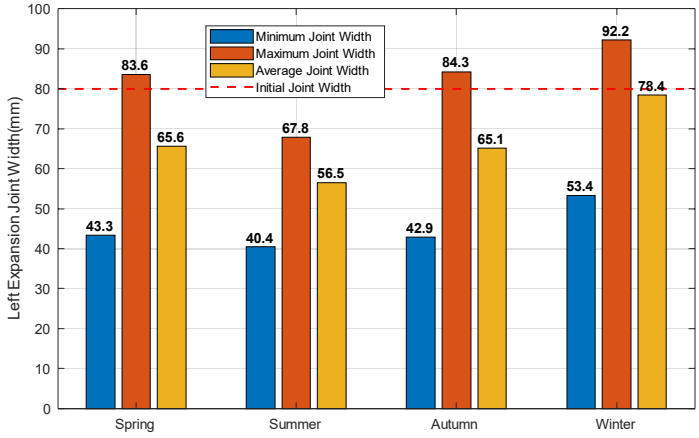

Fig. 9. Variation in Single Expansion Joint Width

As the main girder expands and contracts, the width of the expansion joint also varies, experiencing an increase or decrease. The width of modular expansion joints exhibits a lag effect due to temperature changes, with extrema occurring approximately 2 hours after peak temperatures. Overall, the expansion joint movement generally corresponds to temperature fluctuations. When temperatures decrease, the girder contracts, resulting in an increased joint width, which reaches its maximum after a certain delay during winter's lowest temperatures; conversely, the opposite occurs when temperatures rise. The temperature difference between summer highs and winter lows is the largest, with a maximum joint width change of 51.8mm. Therefore, the girder's expansion and contraction between winter and summer is a key factor in selecting expansion joint devices for bridges.

3.2 Dynamic Response Trend of Expansion Joints

Rends in Dynamic Deflection and Vertical Acceleration.

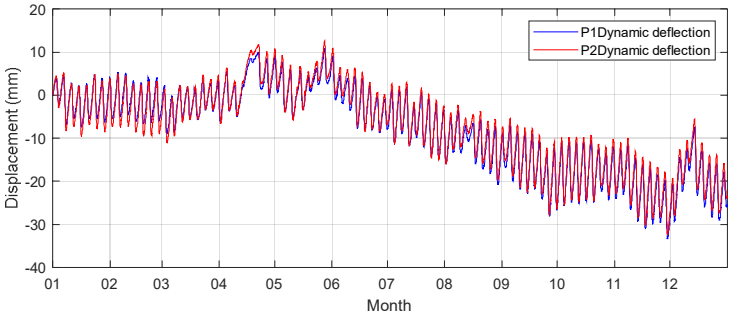

Fig. 10. Annual Variation of Dynamic Deflection at P1 and P2 Measurement Points of the Expansion Joint

From **Fig. 10**, it can be observed that the dynamic deflection shows a general downward trend throughout the year, with variations ranging roughly between -33 mm and +12 mm. The dynamic deflection response of the expansion joint exhibits periodic fluctuations corresponding to seasonal temperature changes, along with a certain lag effect. In late winter to early spring (January to March), the deflection at P2 exceeds that at P1. By March, the waveforms at both points overlap significantly, showing small amplitudes. In April, the amplitude slightly increases, and P1's deflection begins to surpass P2's with minor delays. During summer, the main girder elongates, reducing the expansion joint width to 40.4mm to 67.8mm, resulting in minimal vehicle-induced dynamic response and the lowest equivalent force distribution coefficient, with deflection amplitudes within ±10mm and stable deflection by summer's end. In autumn, deflection continues to decrease steadily. In winter, as the main girder contracts, the joint width increases to 53.4mm to 92.2mm, leading to the highest dynamic response and equivalent force distribution coefficient, with deflection amplitudes ranging from -8mm to -33mm. Special attention is required for vertical displacement of the expansion joints in summer and winter to prevent excessive deflection from affecting the structure.

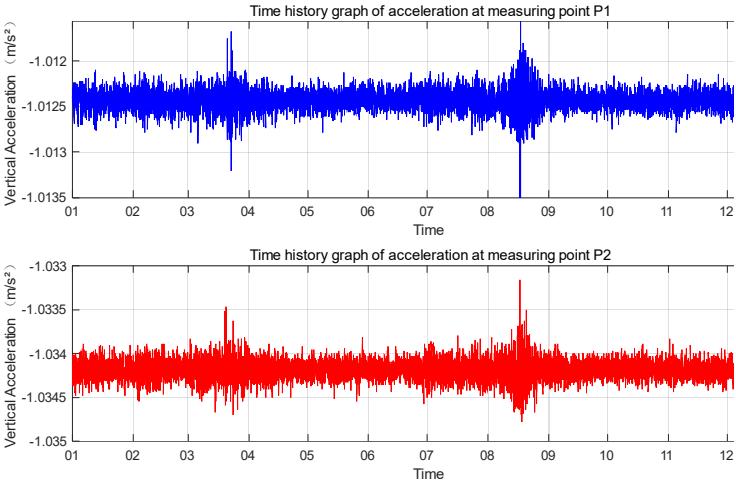

Fig. 11. Annual Variation of Vertical Acceleration at P1 and P2 Measurement Points of the Expansion Joint

Fig. 11 illustrates the vertical acceleration time-history curves for measurement points P1 and P2, covering the complete time series from January to December 2023. The vertical acceleration response of the expansion joint exhibits periodic fluctuations. However, the impact of seasonal temperature variations on vertical acceleration is minimal, with values at both P1 and P2 remaining below -0.001 m/s², indicating stable vertical movement of the modular expansion joint throughout the monitoring period. Notably, significant peaks in vertical acceleration were observed at both points in March and August, suggesting substantial external influences or sudden events during these periods.

Comparison of Dynamic Response Characteristics at Different Measurement Points. The deflection trends at measurement points P1 and P2 are similar, showing significant periodicity. The P2 point exhibits greater amplitude, indicating pronounced vertical fluctuations at the center of the expansion joint, while P1 shows smaller amplitude, suggesting more subdued deflection changes at the ends, likely due to reduced vehicle impacts.

The P1 waveform predominantly displays minor amplitude fluctuations, with vertical acceleration ranging from -1.013 m/s² to -1.012 m/s². In contrast, P2 shows a more stable amplitude, fluctuating between -1.0345 m/s² and -1.0338 m/s². The differences reflect the distinct positions of the measurement points, yet both maintain stable vertical movement throughout the monitoring period.

4 Discussion

4.1 Impact of Seasonal Temperature on the Dynamic Deflection Response of Expansion Joints

Due to the different time spans and sampling frequencies between the annual temperature data and the dynamic deflection and vertical acceleration data, it is necessary to perform interpolation or alignment on the data. Currently, 8784 temperature data points, representing 366 days and 24 hours, are selected and plotted against the dynamic deflection data in a scatter plot to more intuitively observe the relationship between the two.

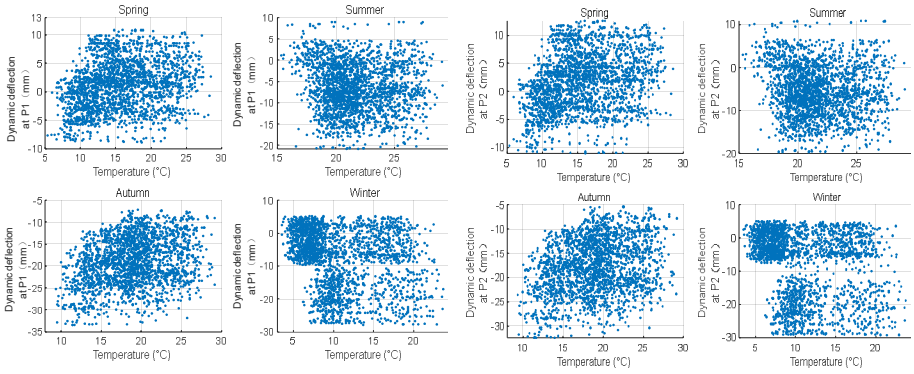

Fig. 12. Scatter Plot of Seasonal Temperature Variation versus Dynamic Deflection Response at P1 and P2 Measurement Points of the Expansion Joint

From **Fig. 12**, it can be observed that in spring, the temperatures range from 10°C to 27°C, with P1 and P2 dynamic deflections between -10mm and 10mm; P2 is generally larger than P1, and data points are dispersed, showing no significant linear relationship between temperature and deflection. In summer, temperatures range from 15°C to 27°C, and dynamic deflections range from -20mm to 10mm, with data concentrated around 20°C. Although dynamic deflection slightly decreases with increasing temperature, the change is not significant. In autumn, temperatures range from 10°C to 27°C, with P1 and P2 deflections between -30mm and -5mm, displaying an even distribution. In winter, temperatures range from 5°C to 20°C, and dynamic deflections range from -30mm to 5mm, with data concentrated in lower temperature zones, showing a clear negative trend as temperatures decrease.

Among the seasons, winter exhibits a notable negative correlation between temperature and dynamic deflection, with lower temperatures increasing negative deflections. In spring and autumn, relationships appear random with no significant correlation, while summer shows a slight decreasing trend in deflection at higher temperatures, though this trend is weak.

4.2 Impact of Seasonal Temperature on Vertical Acceleration of Expansion Joints

Currently, 8784 temperature data points representing 366 days and 24 hours are selected and plotted against the vertical acceleration data in a scatter plot to visually observe the relationship between the two.

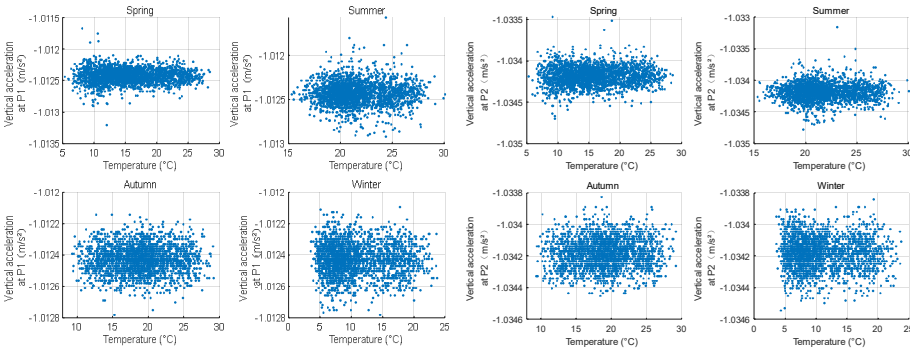

Fig. 13. Scatter Plot of Seasonal Temperature Variation versus Vertical Acceleration Response at P1 and P2 Measurement Points of the Expansion Joint

From **Fig. 13**, it can be observed that from spring to winter, despite significant temperature variations (ranging from 5°C to 27°C), the vertical acceleration at both P1 and P2 (P1: -1.013 m/s² to -1.012 m/s²; P2: -1.0345 m/s² to -1.034 m/s²) shows a limited range of change, and the data points are relatively concentrated. No clear trend related to seasonal temperature changes is evident. Particularly in the low-temperature range of winter (5°C to 10°C), although the data points are somewhat more concentrated, the overall stability of vertical acceleration remains high and is not significantly affected by temperature. This suggests that temperature may not be the primary factor influencing changes in vertical acceleration, and other potential factors might have a more significant impact. Therefore, it can be inferred that variations in vertical acceleration are governed by a combination of complex factors rather than by temperature alone.

5 Conclusion

Compared to previous studies, this research integrates real-time monitoring data with temperature variation analysis, revealing the characteristics of dynamic responses of modular expansion joints induced by vehicles as they vary with seasonal temperature changes. This study addresses the research gap regarding the impact of seasonal temperature differentials on the dynamic responses of expansion joints. The findings indicate:

(1). The equivalent force distribution coefficients for different expansion joint widths were derived, showing that a larger joint width results in a higher coefficient for

the joint's main beam. The cumulative effect of thermal expansion leads to maximum joint width changes of 51.8 mm between summer highs and winter lows.

(2). Under normal operational conditions, the dynamic deflection response of the modular expansion joints is significantly influenced by seasonal temperature variations, exhibiting periodic fluctuations and lag effects. The deflection changes at different measurement points show strong synchronicity, with minimum deflection amplitudes in summer and maximum in winter; autumn and winter deflections are generally greater than those in spring and summer. Vertical fluctuations at mid-span measurement points are significantly higher than at the ends.

(3). The vertical acceleration response of the expansion joints is concentrated in spring and summer, while it is more dispersed in autumn and winter. Throughout the monitoring period, the range of vertical acceleration responses is limited, showing no significant correlation with seasonal temperature changes, indicating high stability across seasons.

This study primarily analyzes monitoring data from a single bridge, which does not comprehensively reflect the behavior of expansion joints in other types of bridges. Future research should focus on long-term monitoring of various bridge types and expansion joints across multiple locations, as well as investigate the influence of other environmental factors (such as humidity and wind speed) on the dynamic response of expansion joints to enhance the generalizability and applicability of the findings.

References

1. Yang X, Zhou Y, et al. Effect of temperature changes on bearing motion of long-span steel truss continuous girder bridge [J]. Construction and Building Materials, 2024, 430. DOI:10.1016/J. CONBUILDMAT. 2024.136440.
2. Hou J, Xu W, et al. Typical diseases of a long-span concrete-filled steel tubular arch bridge and their effects on vehicle-induced dynamic response[J]. Frontiers of Structural and Civil Engineering, 2020, 14(4):867-887. DOI: 10. 1007/s11709-020-0649-9.
3. El-Feky Mohamed H, Elsisi Alaa A, et al. Computer simulation for the seismic behaviour of bridge expansion joints enhanced with SMA: Case study[J]. Case Studies in Construction Materials, 2024, 20. DOI:10. 1016/j. cscm. 2023.e02782.
4. Ji W, Shao T Y, et al. Analytical Investigation of Fatigue Behavior in a Modified Composite Steel Box Concrete Girder Bridge with Corrugated Steel Webs under Pavement and Expansion Joint Deterioration [J]. Journal of Bridge Engineering, 2024,29(10): 04024078. DOI:10.1061/JBENF2.BEENG-6886.
5. Liang Q F, Zhang X B, et al. Bridge Facility Deformation Monitoring Based on Multi-Temporal InSAR Technology [J]. Urban Survey, 2023, (06): 135-140.DOI: 10.3969/ j.issn. 1672-8262.2023.06.031.
6. Li S J, Xin J Z, et al. Separation Method for Temperature Effects in Bridge Deflection Monitoring Data Based on VMD-KLD[J]. Vibration and Shock, 2022, 41(05): 105-113. DOI: 10.13465/j.cnki.jvs.2022.05.015.
7. Shen H P, Chen X J, et al. Analysis Method for Vehicle-Bridge Coupling Vibration Considering Pavement Irregularities[J]. Journal of Army Engineering University, 2023, 2(05): 84-92. DOI: CNKI: SUN: JFJL.0.2023-05-011.

8. Xu W B W B E A. Journal of Southeast University (Natural Science Edition), 2022, 02(52):212-221.
9. Xie J J, Li J, et al. Dynamic Response Analysis of Vehicles Crossing Bridges Considering the Randomness of Pavement Irregularities[J]. Vibration and Shock, 2021, 40(14): 299-306. DOI: 10.13465/j.cnki.jvs.2021.14.039.
10. MOT. General code for design of highway bridge sandculverts:JTGD60—2015[S].Beijing: China Communications Press,2015.
11. Wang X Z, Miao C L, et al. An Analysis on the Thermal Expansion Displacement of Concrete Bridge by 3D Laser Scanning Technology[J]. Academic Journal of Engineering and Technology Science,2021,4(1):70-75.DOI: 10. 25236/AJETS.2021.040107.
12. Huang H B, Yi T H, et al. New Representative Temperature for Performance Alarming of Bridge Expansion Joints through Temperature-Displacement Relationship [J]. Journal of Bridge Engineering, 2018, 23(7): 04018043.1-04018043.14.DOI: 10. 1061 /(ASCE)BE.1943-5592.0001258.